



Supporting Information

for *Small*, DOI: 10.1002/smll.202200975

Holographic Manipulation of Nanostructured Fiber Optics
Enables Spatially-Resolved, Reconfigurable Optical
Control of Plasmonic Local Field Enhancement and
SERS

Liam Collard, Filippo Pisano, Di Zheng, Antonio Balena,
Muhammad Fayyaz Kashif, Marco Pisanello, Antonella
D'Orazio, Liset Mde la Prida, Cristian Ciraci, Marco
Grande, Massimo De Vittorio,* and Ferruccio Pisanello**

Supporting Information

Holographic manipulation of nanostructured fiber optics enables spatially-resolved, reconfigurable optical control of plasmonic local field enhancement and SERS

Liam Collard ^{},[†], Filippo Pisano [†], Di Zheng, Antonio Balena, Muhammad Fayyaz Kashif, Marco Pisanello, Antonella D'Orazio, Liset M. de la Prida, Cristian Ciraci, Marco Grande, Massimo De Vittorio^{*,‡}, Ferruccio Pisanello^{*,‡}*

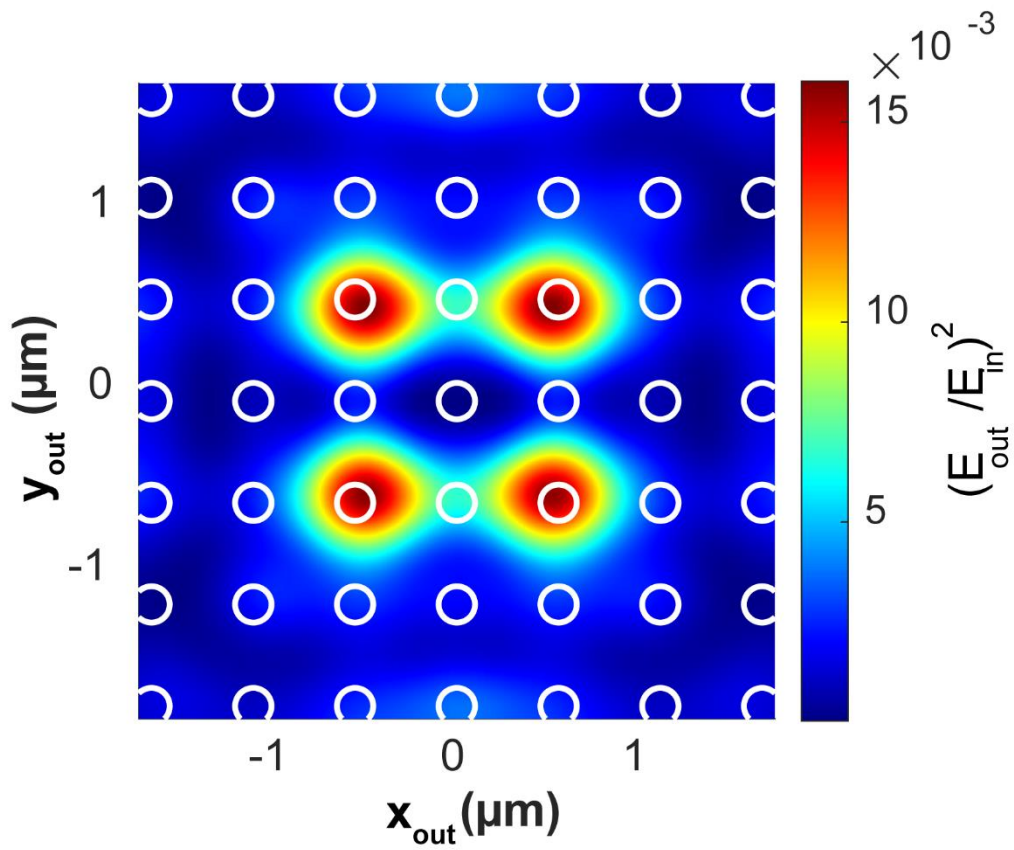


Figure. S1. -3D-FDTD simulations of normal incidence 633 nm transmittance through nanohole arrays (periodicity = 560 nm, hole diameter = 100 nm, gold thickness = 100 nm, spot diameter = 3.5 μm , (intensity is normalized to input value).

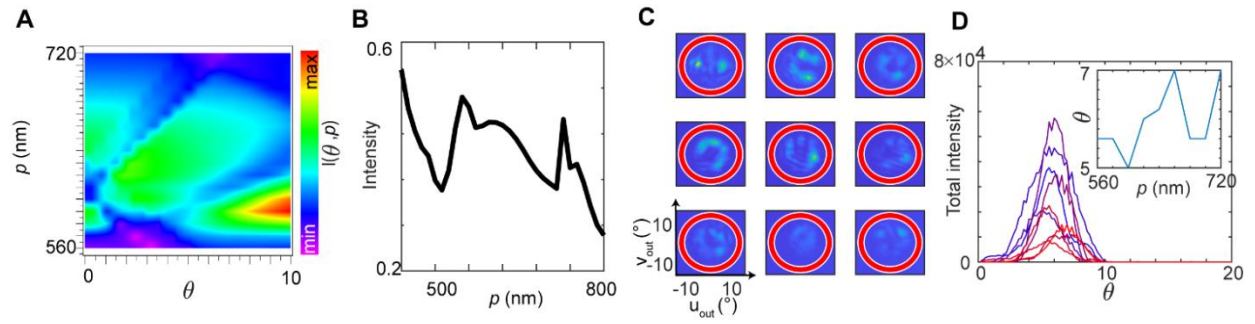


Figure. S2. – A) Simulated transmittance of 633 nm light ($I(\theta, \rho)$) through variable periodicity at different incident angles (gold thickness 100 nm, hole diameter 100 nm). B) Integral of $I(\theta, \rho)$ along θ , from the data in panel A. C) Images of the corresponding Fourier plane transmission of 9 wavefront shaped spots on the plasmonic output facet exciting each of the 9 nanohole arrays. D) The shifting position of the maximum of $|\mathbf{k}_t|$.

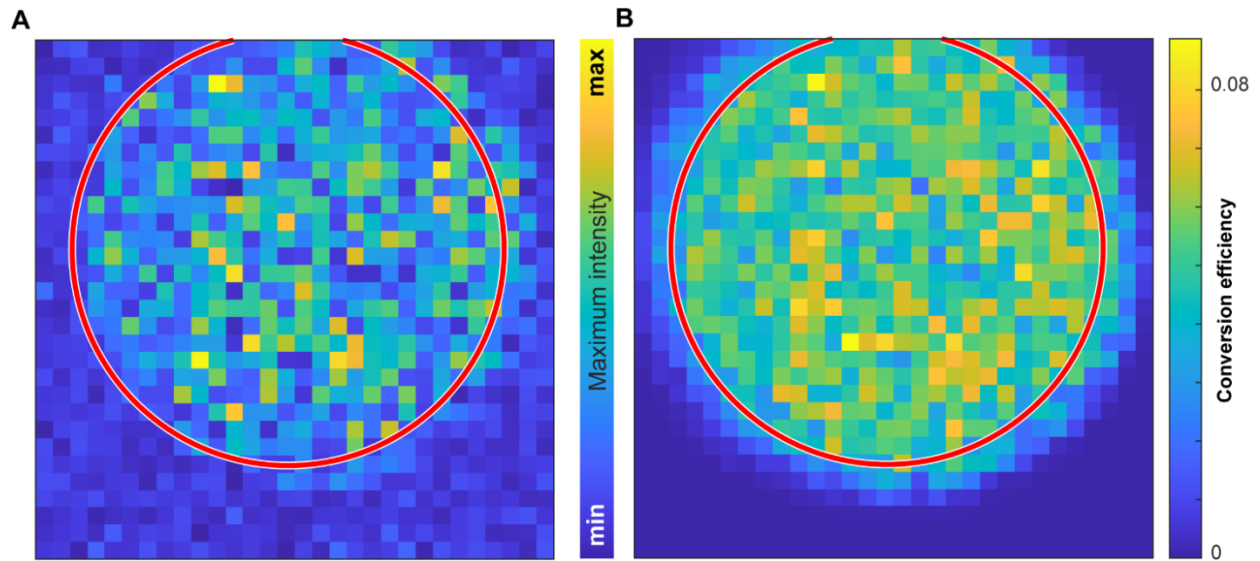


Figure. S3. – A) Maximum intensity for 30 by 30 array of focused spots generated through a standard silica MMF (NA 0.22 , core diameter 50 μm). Red circle represents the boundaries of the fiber core. B) Conversion efficiency of each foci (ratio of modulated light to unmodulated). The dark spots correspond to blind parts of the reference beam

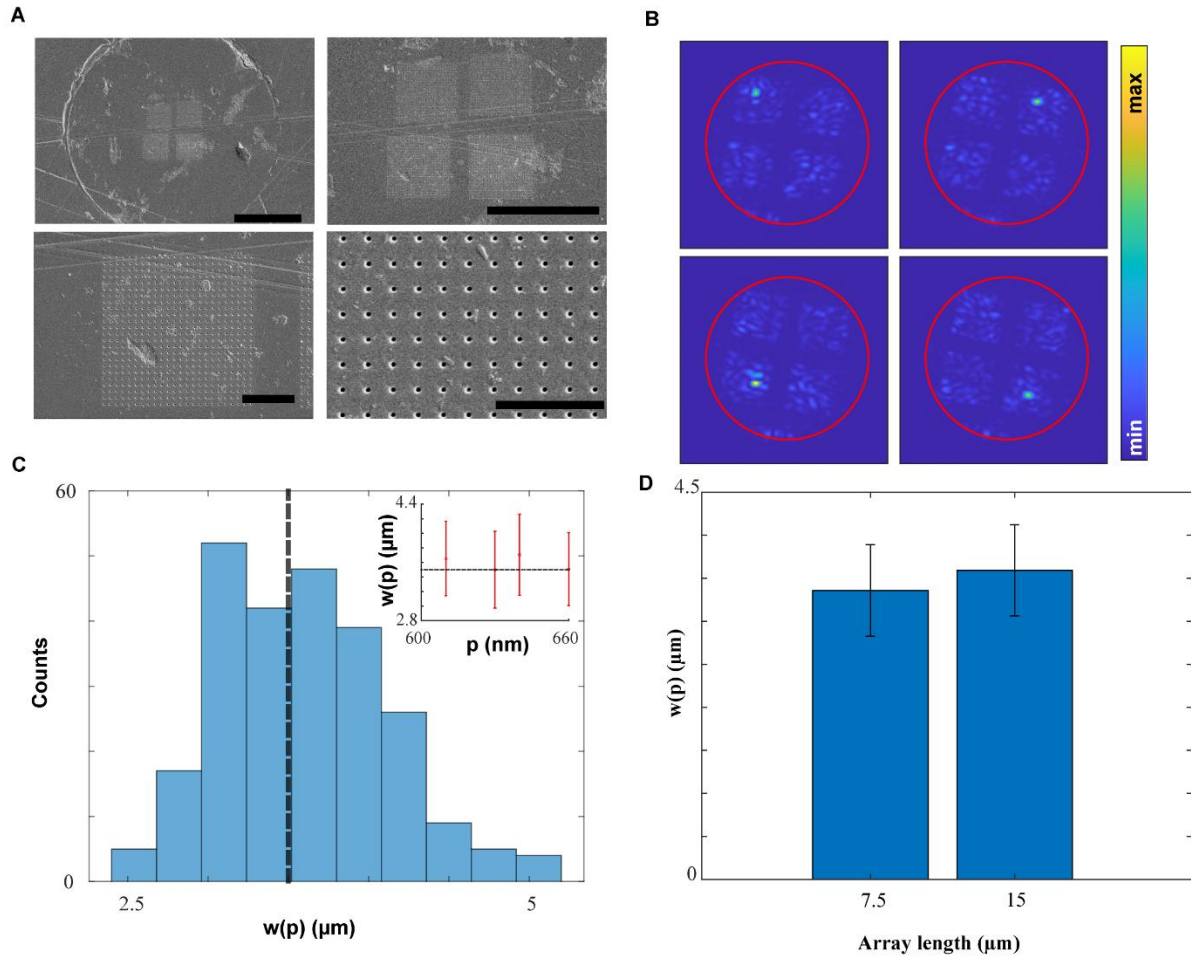


Figure S4 A) SEM images of fiber facet with four 15x15 μm nanohole arrays milled. Scale bars are 40 μm, 20 μm, 5 μm and 2.5 μm. The nanoholes were 100 nm wide and the gold layer 100 nm thick. B) Focused spots generated with the wavefront engineering system shown in figure 1 (main text) on each of the four nanohole arrays. C) Histogram of measured spot width ($1/e^2$) for a set of spots generated on all four nanohole arrays. The inset shows the average width of the foci on each structure. Black lines show the theoretical limit from the fibers NA. D) Comparison of the average foci width generated on nanohole arrays of 7.5x7.5 μm and 15x15 μm.

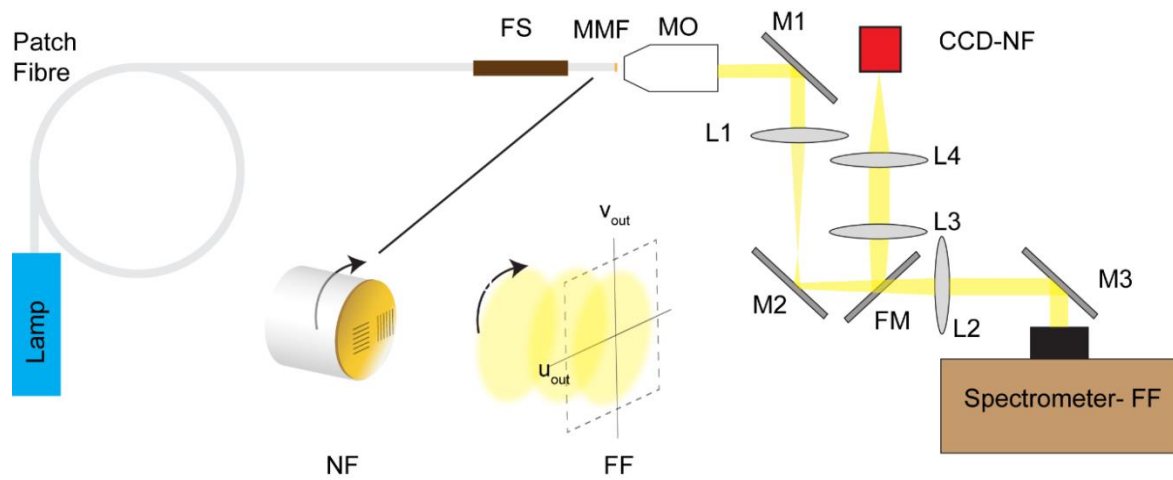


Figure. S5. – FS – fiber sleeve, MMF – multimode fiber, MO – microscope objective, M- mirror, L - Lens, FM – Flip mirror, CCD-NF – charged coupling device.

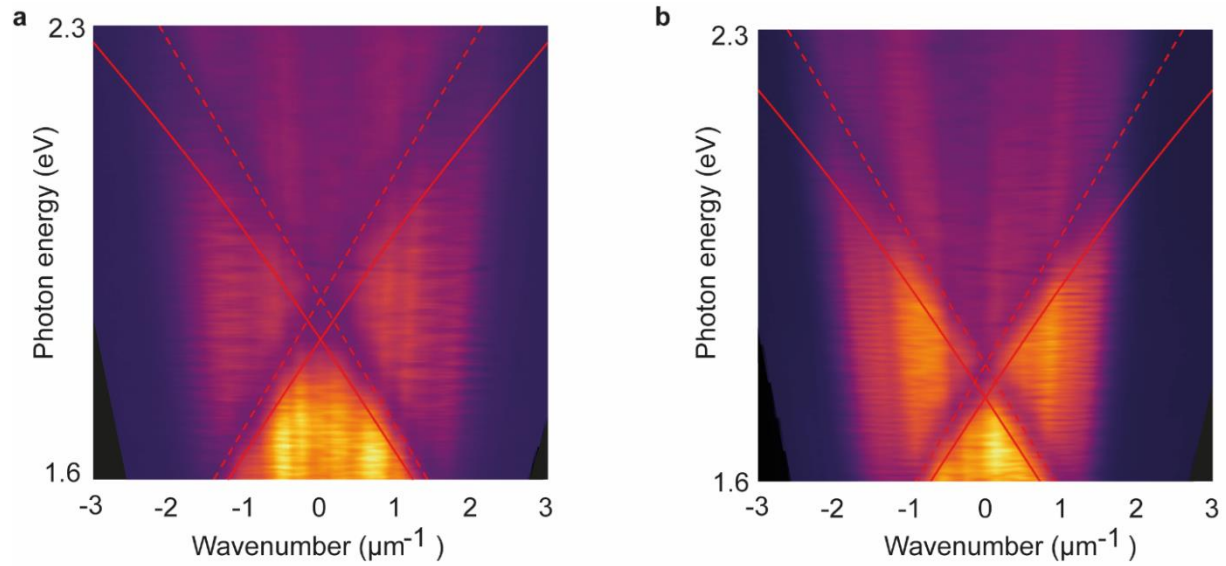


Figure. S6. - Dispersion diagrams in photon energy (eV) vs wave-vector (μm^{-1}) units for the two nanogratings milled on the fiber facet, as shown in figure 3. Panel (a) refers to G1, while panel (b) refers G2 when measured along the u and v axis in the Fourier plane, respectively. The continuous lines show the predicted dispersion of a Surface Plasmon Resonance at the gold-air interface, while the dashed lines show the wood anomalies calculated for a periodicity of 635 nm for grating G1 and 660 nm for G2.

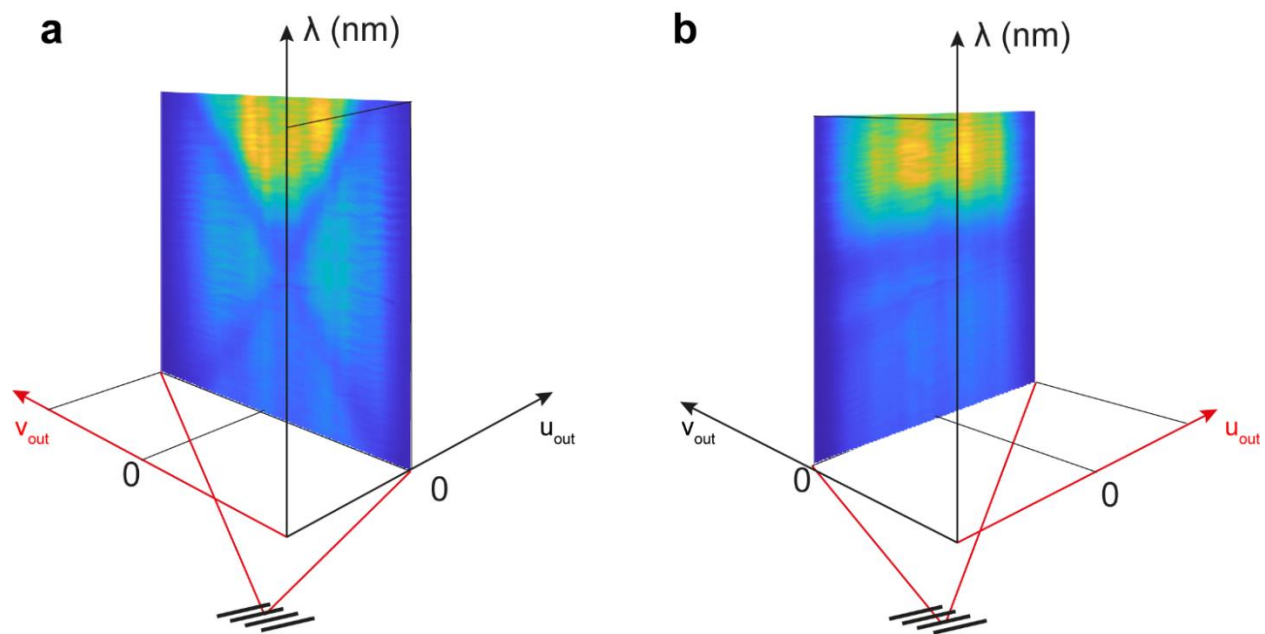


Figure. S7. – Illustration of measurement of dispersion of G1 along u_{out} and v_{out} .

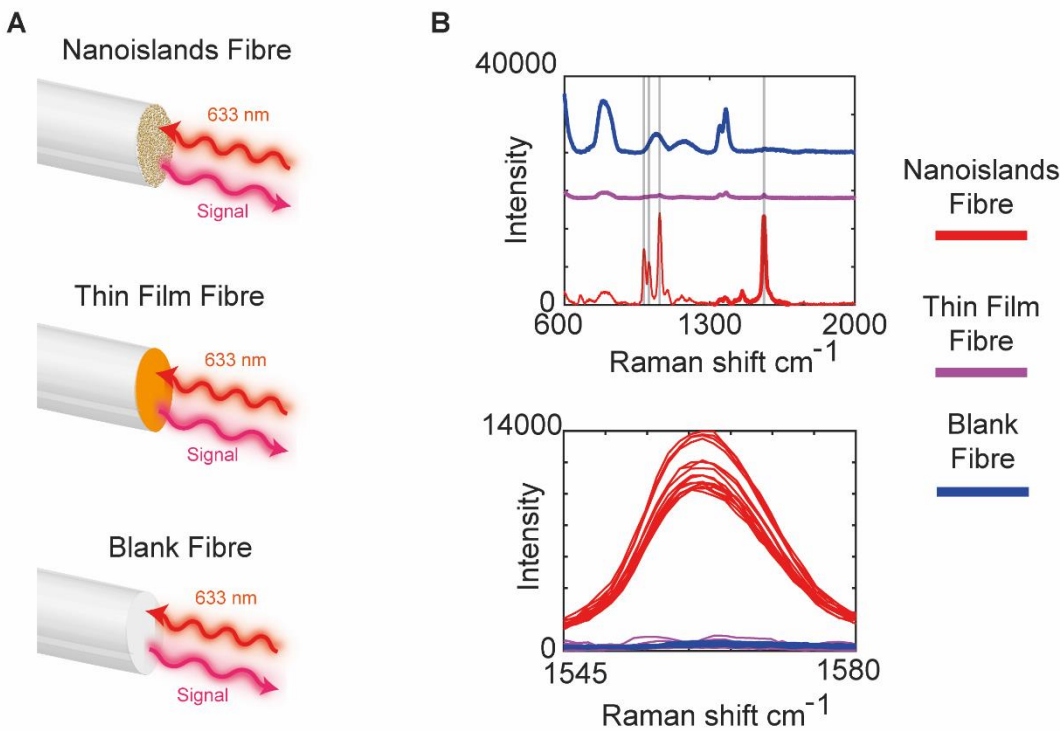


Figure. S8. – Comparison between Raman signal by direct excitation of the fiber facet. (A) Illustration of direct excitation of Raman scattering/SERS from BT molecules functionalized on blank, gold coated and NIs-covered fiber facet. (B) Detected spectra for the three configurations in panel A (excitation power was 1 mW), with a zoom on the 1562 cm^{-1} BT molecule peak.